

Limiting vertical acceleration for ride comfort in active suspension systems

Proc IMechE Part I:
J Systems and Control Engineering
2018, Vol. 232(3) 223–232
© IMechE 2017
Reprints and permissions:
sagepub.co.uk/journalsPermissions.nav
DOI: 10.1177/0959651817745469
journals.sagepub.com/home/pii


Fabian León-Vargas¹ , Fabricio Garelli² and Mauricio Zapateiro³

Abstract

This article proposes a new adaptive control algorithm for active suspension systems of passenger cars. It combines a proportional–integral–derivative controller for suspension deflection together with a sliding mode reference conditioning outer loop that uses the vertical acceleration of the car body as a complementary source of control. The proposed approach is software-based and allows setting up limit values to critical variables, such as the vertical acceleration, which can be directly tuned by the system designer to range from the original proportional–integral–derivative response to other ones with tighter control on the constrained variable. A longitudinal half-car system subject to irregular excitation from a road surface is used for assessment. The proposed proportional–integral–derivative with sliding mode reference conditioning is compared to the same proportional–integral–derivative controller without the outer conditioning loop, as well as with a passive suspension system. International standards on overall vibration magnitudes are used to quantify the differences obtained in this assessment. Results obtained from the proposed control system show better performance and handle trade-offs, improving the ride comfort without adversely affecting the road holding of the car.

Keywords

Active suspension system, sliding mode reference conditioning, road comfort, half-car

Date received: 14 July 2017; accepted: 30 October 2017

Introduction

Car suspension systems is an important research topic with significant developments in the last decades as they play an important role for improving ride comfort, road holding, and performance characteristics of a car.¹ Suspension systems can be classified as passive, semi-active, and active according to the tuning possibilities that their components offer. Passive suspension systems are still the most used alternative but they are limited in improving ride comfort, road holding or suspension deflection as the compromise of these criteria with each other is highly conflicting, which demands variable spring and damper characteristics.² Semi-active suspension systems implement variable damping characteristics representing a considerable improvement over passive suspension systems. They can be adjusted in real time to provide better suspension by absorbing energy, but they cannot inject energy to the system. This is an advantage since semi-active suspension cannot lead to instability.³

Active suspensions have remained attractive for many years in both academia and industry for improving car ride comfort and road holding performance. An active suspension system can employ a kind of

suspension force generation such as a pneumatic or hydraulic actuator that is placed between the car body (CB) and wheel–axle parallel to the suspension elements.^{1,4} Although active suspensions are able to both add and dissipate energy from the system, there are still conflicts in the requirements design. Enhancing ride comfort with a firm uninterrupted contact of the wheels to road without producing a large dynamic tire load in order to avoid exceeding suspension deflection is a big challenge. This stands as a compromise between car safety and ride comfort. Moreover, the overall performance of the active suspension system is affected by inherent suspension movements.² Therefore, achieving good related trade-offs is the basis for successfully designing an active suspension control system.

¹Research Group in Energy and Materials, Facultad de Ingeniería Mecánica, Universidad Antonio Nariño, Bogotá, Colombia

²Universidad Nacional de La Plata, La Plata, Argentina

³EDMA Innova, Girona, Spain

Corresponding author:

Fabian León-Vargas, Research Group in Energy and Materials, Facultad de Ingeniería Mecánica, Universidad Antonio Nariño, Calle 22 Sur No. 12D-81, Bogotá 111311, Colombia.
Email: fabianleon@uan.edu.co

In order to overcome suspension system trade-offs and performance limitations, some active suspension control approaches have been proposed. Linear quadratic regulator,⁵ backstepping control,^{2,6} and fuzzy control^{7–10} are some of the most recurrent techniques applied in this field. Moreover, intelligent methodologies based on neural networks and genetic algorithms,¹ as well as robust controllers,¹¹ H_∞ control,^{12–14} and other control strategies^{15–17} have also been developed with good performance results. However, classical proportional–integral–derivative (PID) controllers have also been considered in different works,^{18,19} some of them implementing iterative learning algorithms to obtain optimum PID controller parameters.²⁰

In recent years, a new control strategy named sliding mode reference conditioning (SMRC) has been developed and applied successfully to constrained dynamical systems in several control problems such as pitch control in wind turbines,²¹ robot path tracking²² or artificial pancreas,²³ among others. This method follows the two-step approximation to constrained control providing a rigorous methodology design with robustness against disturbances, implementing the variable structure systems theory through a transient sliding regime to satisfy system constraints.²⁴

Some approaches for active suspension systems considering conventional sliding mode (SM) control as in the study of Sam and Osman²⁵ or in Zhao et al.²⁶ can be found commonly in the literature. Recently, Wang et al.²⁷ proposed a super-twisting algorithm (STA) based finite-time SM tracking control scheme, which is a novel extended super-twisting disturbance observer for compensating the uncertainties. In contrast, in our proposal, SMs are not established within the main control loop but in an external software-based loop. In this manner, an outer control loop is added to the main closed-loop controller so as to impose constraints on the CB vertical acceleration. As can be found in previous implementations,^{21–23} the main controller can be of any nature.

In this article, a new control strategy for active suspension systems using a PID controller as the principal control for suspension deflection and the CB vertical acceleration as the complementary source of control for the SMRC algorithm is proposed. The suspension system model is modeled by a longitudinal half-car system with 4 degrees of freedom (DOF), which is evaluated with a bump excitation from a road surface. Performance exhibited by this active control system is compared to its counterpart without the auxiliary SMRC algorithm, as well as with the passive suspension system. International standards on overall vibration magnitudes are used to quantify the differences obtained in this assessment.

This article is organized as follows. A half-car suspension model used for controller design and assessment of active suspension systems is formulated in section “Half-car suspension model.” Section “Performance specifications” presents the performance

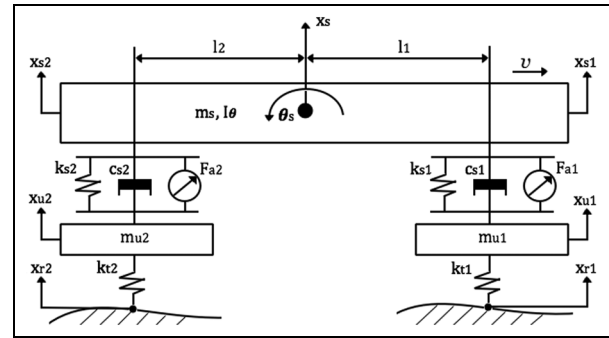


Figure 1. Half-car model with active suspension system.

specifications considered as trade-offs in this problem.” The controller design and the basis of the SMRC strategy are given in section “Controller design.” Results and discussion are presented in section “Results and discussion” and the article conclusion in section “Conclusion.”

Half-car suspension model

Figure 1 shows the model of a half-car suspension represented as a linear 4-DOF system. It is composed of a single sprung mass (CB) linked to two unsprung masses (front/rear wheels). Passive suspensions are modeled as linear viscous dampers and spring elements, while the compressibility of wheels pneumatic is modeled as springs without damping dynamics. In addition to passive suspensions, servo-hydraulic actuators are considered between the sprung and unsprung masses to provide active forces.

Assuming a pitch angle $\theta_s(t)$ (i.e. the rotary angle of the CB at the center of gravity) small enough, from Figure 1, results evident that the displacements of the sprung mass can be considered as

$$\begin{aligned} x_{s1}(t) &= x_s(t) + l_1 \sin \theta_s(t) \approx x_s(t) + l_1 \theta_s(t) \\ x_{s2}(t) &= x_s(t) - l_2 \sin \theta_s(t) \approx x_s(t) - l_2 \theta_s(t) \end{aligned} \quad (1)$$

where $x_{s1}(t)$ and $x_{s2}(t)$ are the vertical displacements of the CB at the front/rear suspension locations, l_1 and l_2 are the lengths of the front/rear suspension locations respect to to the center of gravity of the CB ($l_1 + l_2 = l$) and $x_s(t)$ is the displacement of the center of mass. The equations of motion for the CB and the front/rear wheels for the half-car suspension model are given by

$$\begin{aligned} m_s \ddot{x}_s(t) + k_{s1}[x_{s1}(t) - x_{u1}(t)] + c_{s1}[\dot{x}_{s1}(t) - \dot{x}_{u1}(t)] + \\ k_{s2}[x_{s2}(t) - x_{u2}(t)] + c_{s2}[\dot{x}_{s2}(t) - \dot{x}_{u2}(t)] = \\ F_{a1}(t) + F_{a2}(t) \end{aligned} \quad (2)$$

$$\begin{aligned} I_\theta \ddot{\theta}_s(t) - l_1 k_{s1}[x_{s1}(t) - x_{u1}(t)] - l_1 c_{s1}[\dot{x}_{s1}(t) - \dot{x}_{u1}(t)] + \\ l_2 k_{s2}[x_{s2}(t) - x_{u2}(t)] + l_2 c_{s2}[\dot{x}_{s2}(t) - \dot{x}_{u2}(t)] = \\ l_1 F_{a1}(t) - l_2 F_{a2}(t) \end{aligned} \quad (3)$$

$$m_{u1}\ddot{x}_{u1}(t) - k_{s1}[x_{s1}(t) - x_{u1}(t)] - c_{s1}[\dot{x}_{s1}(t) - \dot{x}_{u1}(t)] + k_{t1}[x_{u1}(t) - x_{r1}(t)] = -F_{a1}(t) \quad (4)$$

$$m_{u2}\ddot{x}_{u2}(t) - k_{s2}[x_{s2}(t) - x_{u2}(t)] - c_{s2}[\dot{x}_{s2}(t) - \dot{x}_{u2}(t)] + k_{t2}[x_{u2}(t) - x_{r2}(t)] = -F_{a2}(t) \quad (5)$$

and the constraints are given by¹²

$$x_s(t) = \frac{l_2 x_{s1}(t) + l_1 x_{s2}(t)}{l} \quad (6)$$

$$\theta_s(t) = \frac{x_{s1}(t) - x_{s2}(t)}{l} \quad (7)$$

where m_s is the CB mass, I_θ is the pitch moment of inertia respect to the center of mass, and subindex i valued as 1 or 2 to indicate the front or rear side, respectively; m_{ui} is the unsprung mass on the front/rear wheel, $x_{ui}(t)$ is the front/rear unsprung mass vertical displacement, $x_{ri}(t)$ is the front/rear road surface displacement, k_{si} is the spring stiffness of the front/rear suspension, k_{ti} is the front/rear tire stiffness, and c_{si} is the damping coefficient of the front/rear suspension. Similarly, $F_{ai}(t)$ is the front/rear actuator force input.

Equations (2)–(5) can be rewritten as

$$M\ddot{\mathbf{x}}(t) + C\dot{\mathbf{x}} + K\mathbf{x}(t) = P\mathbf{x}_r(t) + L\mathbf{F}_a(t) \quad (8)$$

where the state, excitation vectors, and active control are, respectively, given by

$$\begin{aligned} \mathbf{x}(t) &= [x_{s1}(t), x_{u1}(t), x_{s2}(t), x_{u2}(t)]^T, \\ \mathbf{x}_r(t) &= [x_{r1}(t), x_{r2}(t)]^T, \\ \mathbf{F}_a(t) &= [F_{a1}(t), F_{a2}(t)]^T \end{aligned} \quad (9)$$

and M , C , K , P , and L are, respectively, denoted as

$$\begin{aligned} M &= \begin{bmatrix} l_2 m_s / l & 0 & l_1 m_s / l & 0 \\ I_\theta / l & 0 & -I_\theta / l & 0 \\ 0 & m_{u1} & 0 & 0 \\ 0 & 0 & 0 & m_{u2} \end{bmatrix} \\ C &= \begin{bmatrix} c_{s1} & -c_{s1} & c_{s2} & -c_{s2} \\ l_1 c_{s1} & -l_1 c_{s1} & -l_2 c_{s2} & l_2 c_{s2} \\ -c_{s1} & c_{s1} & 0 & 0 \\ 0 & 0 & -c_{s2} & c_{s2} \end{bmatrix} \\ K &= \begin{bmatrix} k_{s1} & -k_{s1} & k_{s2} & -k_{s2} \\ l_1 k_{s1} & -l_1 k_{s1} & -l_2 k_{s2} & l_2 k_{s2} \\ -k_{s1} & k_{s1} + k_{t1} & 0 & 0 \\ 0 & 0 & -k_{s2} & k_{s2} + k_{t2} \end{bmatrix} \end{aligned} \quad (10)$$

$$P = \begin{bmatrix} 0 & 0 \\ 0 & 0 \\ k_{t1} & 0 \\ 0 & k_{t2} \end{bmatrix} \quad L = \begin{bmatrix} 1 & 1 \\ l_1 & -l_2 \\ -1 & 0 \\ 0 & -1 \end{bmatrix}$$

Finally, the dynamics of the servo-hydraulic actuator is modeled here as $G_{ai}(s) = 1/(1/75s + 1)$,¹¹ whose input is $F_{ai}(t)$ and the active force to the system as output.

Performance specifications

The following specifications are considered in order to keep real constraints for the system:^{10,12,15,18,28}

1. *Disturbance rejection*—the active suspension controller should maintain the steady-state error close to zero;
2. The *maximum suspension deflection* is limited to physical values in order to avoid damaging car components and prevent deterioration of passenger ride comfort. Therefore, the suspension system must not exceed the limit given as

$$|y_i(t)| \leq z_{max} \quad (11)$$

where $i \in (1, 2)$, $y_i(t) = x_{si}(t) - x_{ui}(t)$, and z_{max} is set to ± 10 cm, under any road disturbance input and car running conditions.

3. The *maximum actuator force* must not exceed the static weight of the car

$$F_{ai}(t) < m_s g \quad (12)$$

where g is the gravity acceleration corresponding to 9.81 m/s^2 .

4. A *good road holding* is achieved when the dynamic tire load transmitted through the road (F_{ti}) not exceed the static tire load, F_{ti}^{stat} , that is

$$F_{ti}(t) \leq F_{ti}^{stat} \quad (13)$$

where

$$F_{ti}(t) = k_{ti}(x_{ui}(t) - x_{ri}(t)) \quad (14)$$

and

$$F_{ti}^{stat} = g \left[\frac{m_s l_i}{l_1 + l_2} + m_{ui} \right] \quad (15)$$

5. The root mean square (RMS) values of performance parameters given by φ_{RMS} , will be used to

enable detailed performance comparison of the active versus passive suspension system

$$\varphi_{RMS} = \sqrt{\frac{1}{T} \int_0^T \varphi^2 \cdot dt} \quad (16)$$

where

$$\varphi = [y_i(t), F_{ii}(t), \dot{x}_s(t), \ddot{\theta}_s(t), F_{ai}(t)]^T \quad (17)$$

6. The *ride comfort* is assessed from the CB vertical acceleration, which needs to be minimal for good ride comfort within the low-frequency band of 0.1–10 Hz. The frequency-weighted RMS acceleration described on ISO 2631-1:1997 is the basis for evaluation of car ride comfort.²⁹ In this work, the active suspension system model does not include car seats and therefore W_k , the ISO 2631-1:1997 frequency weighting for acceleration input at the feet, is used.

A fifth-order approximation of W_k is expressed in the study of Zuo and Nayfeh³⁰ as

$$W_k(s) = (87.72s^4 + 1138s^3 + 11336s^2 + 5453s + 5509) \times (s^5 + 92.6854s^4 + 2549.83s^3 + 25969s^2 + 81057s + 79783)^{-1} \quad (18)$$

from which the weighted RMS acceleration, a_w^{RMS} , is given by

$$a_w^{RMS} = \sqrt{\frac{1}{T} \int_0^T (W_k(\ddot{x}_s(t)))^2 \cdot dt} \quad (19)$$

A vibration-induced discomfort scale for various values of a_w^{RMS} , given by the ISO 2631-1:1997,²⁹ is presented in Table 1.

Controller design

SMRC

The concept of reference conditioning to achieve a realizable reference arises in the context of constrained

Table 1. Magnitudes of overall vibration according to ISO 2631-1:1997.

Frequency-weighted vibration magnitude (RMS)	Likely reaction in public transport
Less than 0.315 m/s ²	Not uncomfortable
0.315–0.63 m/s ²	A little uncomfortable
0.5–1 m/s ²	Fairly uncomfortable
0.8–1.6 m/s ²	Uncomfortable
1.25–2.5 m/s ²	Very uncomfortable
Greater than 2 m/s ²	Extremely uncomfortable

RMS: root mean square.

control systems. Specifically, Garelli et al.²⁴ have used the SMRC strategy in a robust way to get realizable references in several applications considering restrictions in the actuator, in the outputs, or in any system state.^{21–23}

Constraints are fulfilled in SMRC schemes varying the reference of the control system through an external sliding control loop instead of representing the main control loop. Unlike conventional variable structure controllers and SMs, the SMRC is considered as a transitional mode of operation, which means that only works when constraints are prone to be surpassed.

A generic version of the SMRC loop is illustrated in Figure 2. Two elements govern its performance: a switching design to fulfill the constraints forcing the system to remain in the allowed region and a filter F designed to smooth out the switching output $\omega(t)$, obtaining $\omega_f(t)$ in order to get a realizable conditioned set-point $r_f(t)$, that is, $r_f(t) = \omega_f(t) + r$. In this scheme, a main control loop of any nature is represented by the block Θ , which originally implements r as set-point. The system outputs $y(t)$ and $v(t)$ represent the main controlled variable and the variable to be bounded, respectively, where $v^*(t)$ is the bound imposed to the system.

The switching logic is implemented as

$$\omega(t) = \begin{cases} \omega^+ & \text{if } \sigma_{SM}(t) > 0 \\ 0 & \text{if } \sigma_{SM}(t) \leq 0 \end{cases} \quad (20)$$

where

$$\sigma_{SM}(t) = v(t) - v^*(t) + \sum_{i=1}^{l-1} \tau_i (v(t)^{(i)} - v^*(t)^{(i)}) \quad (21)$$

with l being the relative degree between the output $v(t)$ and the input $\omega(t)$. $v(t)^{(i)}$ and $v^*(t)^{(i)}$ are the i th derivative of $v(t)$ and $v^*(t)$, respectively. τ_i are constant gains and ω^+ is the $\omega(t)$ upper value. The filter F is implemented as the first-order filter $\dot{w}_f(t) = -\alpha(w_f(t) - \omega(t))$ with α a design parameter.³¹ The parameter α must be fast enough with respect to the dynamics of the original system so as not to affect the tracking of the reference signal r , but not too fast in order to smooth as much as possible the discontinuous action of ω^+ and ω^- . In general, it can be taken 10 times faster than the main system dynamics. If further adjustments of α were desired,

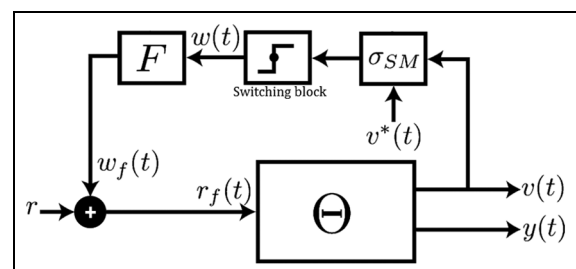


Figure 2. Block diagram of an SMRC loop.

Table 2. PID controller gain values (N/m) for suspension travel and SMRC parameters values.

k_{P1}	k_{I1}	k_{D1}	k_{P2}	k_{I2}	k_{D2}	\bar{x}_s (m/s ²)	\underline{x}_s (m/s ²)	α (s ⁻¹)	ω^+ (m)	ω^- (m)
9450	550	3000	4050	250	2500	1.2	-1.2	1/0.2	-1	1

they would have to be done along with amplitude of w_f so as not to affect the domain of SM existence.²⁴

Note that according to the definition of the switching function in equation (21) and from the transversality condition,²⁴ the conditioning surface $\sigma_{SM}(t)$ has relative degree unitary with respect to $\omega(t)$ (its first derivative explicitly depends on $\omega(t)$), which guarantees the SM establishment.

SMRC adapted for ride comfort

In this study, the SMRC algorithm is applied on active suspension systems to improve the passenger ride comfort, which implies that the CB vertical acceleration ($\ddot{x}_s(t)$) must be attenuated in the face of road disturbances, see section “Performance specifications.” Hence, upper and lower limits in the maximum positive and negative vertical accelerations have to be set. This consideration leads to adapt equation (20), defining the switching logic as

$$\omega(t) = \begin{cases} \omega^+ & \text{if } \bar{\sigma}_{SM}(t) > 0 \\ \omega^- & \text{if } \underline{\sigma}_{SM}(t) < 0 \\ 0 & \text{in othercase} \end{cases} \quad (22)$$

where $\bar{\sigma}_{SM}(t)$ and $\underline{\sigma}_{SM}(t)$ correspond to the SMs-bounded surfaces related to the upper and lower limits of the vertical acceleration, respectively. According to equations (8), (20), and (21), $\ddot{x}_s(t) = f(F_a(t))$ and $F_a(t) = f(\omega_f)$; therefore, the relative degree between the output $\ddot{x}_s(t)$ and the input $\omega(t)$ is zero. Considering that the first-order filter provides a relative degree unitary ($l = 1$), the bounded surface in each case is defined as

$$\begin{aligned} \bar{\sigma}_{SM}(t) &= \ddot{x}_s(t) - \bar{x}_s \\ \underline{\sigma}_{SM}(t) &= \ddot{x}_s(t) - \underline{x}_s \end{aligned} \quad (23)$$

where \bar{x}_s and \underline{x}_s are the upper and lower limits of the vertical acceleration, respectively.

Controller architecture

The controller architecture is composed of a main control loop at each side (front/rear) of the half-car model in order to regulate the suspension deflection y_i and an external loop with the SMRC algorithm to adapt the force demanded by the controller and avoid surpassing the upper \bar{x}_s and lower \underline{x}_s limits of the CB vertical acceleration. In both main control loops, the set-points are set to zero. Figure 3 shows this controller architecture. The PID control algorithm reacts to the corresponding suspension deflection error, and the SMRC smoothed output, ω_f , is derived to each front and rear suspension

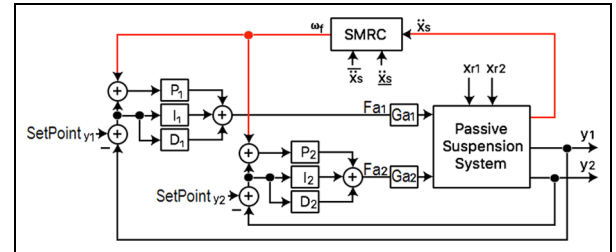


Figure 3. PID control architecture with SMRC for active suspension system.

loop through the reference of the proportional component of each PID. Table 2 presents the PID controller gains and the SMRC parameters values used. These gains were based on applying the Ziegler–Nichols PID controller gains tuning method and on the achievement of results with acceptable performance, while for the SMRC filter, a faster behavior than the suspension system dynamics was considered.

Results and discussion

In this work, a typical bump is used to evaluate the system response to disturbance. This road surface is modeled as

$$x_{r1} = \begin{cases} \frac{a}{2} \left(1 - \cos\left(\frac{2\pi v_0 t}{\lambda}\right) \right), & 1 \leq t \leq 1 + \frac{\lambda}{v_0} \\ 0, & \text{otherwise} \end{cases} \quad (24)$$

where a and λ are the height and the length of the bump, respectively, and v_0 is the car forward velocity. The road condition for the rear wheel x_{r2} is assumed to be the same as the front wheel but with a time delay of $(l_1 + l_2)/v_0$. This sinusoidal bump profile is illustrated in Figure 4.

The numerical values for the model parameters are based on the study of Ekoru and Pedro¹⁸ and are showed in Table 3.

Two active suspension control systems were evaluated, the PID and the PID + SMRC algorithm, and compared with respect to the uncontrolled case (passive).

Figures 5–7 show the passive and active sprung mass vertical acceleration and displacement; the front and rear suspension deflection, unsprung displacement; and control input and dynamic tire obtained, respectively, from the bump test response. Figure 8 shows the SMRC output performed in this test. Table 4 presents the RMS values of the performance variables defined

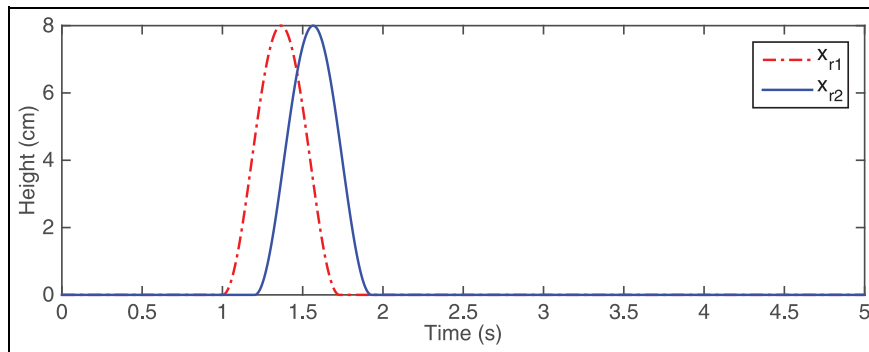


Figure 4. Bump disturbance.

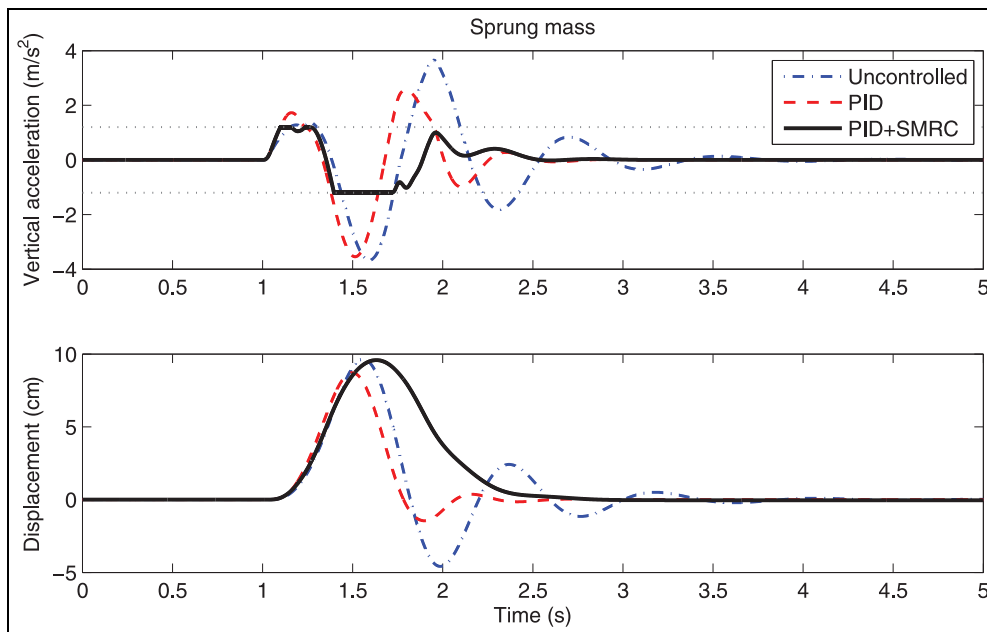


Figure 5. Sprung mass vertical acceleration (top) and displacement (bottom).

Table 3. Parameters of the half-car model suspension system.

Parameters	Value
Sprung mass, m_s	580 kg
Moment of inertia, I_θ	1100 kg.m ²
Front/rear unsprung mass, m_{u1}/m_{u2}	40 kg
Front/rear spring stiffness, k_{s1}/k_{s2}	2.35*10 ⁴ N/m
Front/rear damping coefficient, c_{s1}/c_{s2}	1500/1600 N/m
Front/rear tire stiffness, k_{t1}/k_{t2}	1.90*10 ⁵ N/m
Front/rear distance, l_1/l_2	1/1.5 m
Bump height, a	0.08 m
Wavelength, λ	9.1 m
Car speed, v_0	12.5 m

in section “Performance specifications,” while Table 5 presents the weighted RMS acceleration and the corresponding discomfort level obtained.

Results show that all performance specifications considered in section “Performance specifications” are completely fulfilled using the PID + SMRC

algorithm. Particularly, low frequency of the bump disturbance are more attenuated respect to the PID without SMRC (Figure 5). Results presented in Table 5 show that ISO 2631-1:1997 discomfort level obtained with the PID + SMRC algorithm is at the lowest level of the scale introduced in Table 1. This discomfort level (measured relative to a_w^{RMS}) is 54.3% and 44.4% less respect to uncontrolled and PID control, respectively. However, according to Table 4, the PID + SMRC strategy needs approximately 49.8% more force in average than the PID control. In terms of cost–benefit, this implies that an improved ride comfort demands a greater amount of energy. In the PID + SMRC control algorithm, it is mainly related to the upper and lower limits used in the CB vertical acceleration; a more restricted value for these limits will lead the system to require a higher energy expenditure.

All suspension systems (active and passive) fulfill the maximum suspension deflection constraint (10 cm) for both the front and rear sides, see Figure 6. However,

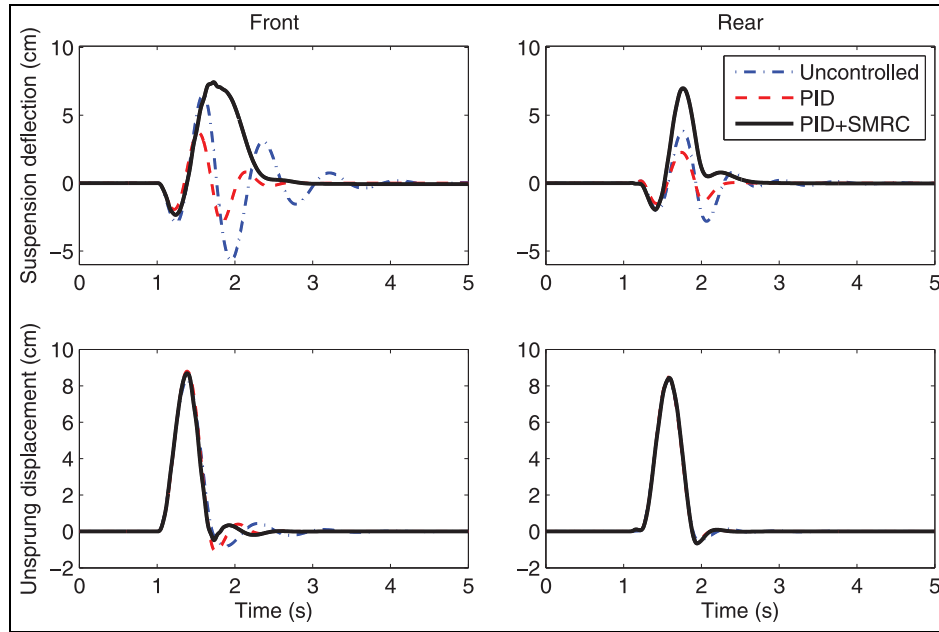


Figure 6. Front and rear suspension deflection (top) and unsprung displacement (bottom).

Table 4. RMS values of the performance metrics from passive and active suspension systems.

	y_1 (m)	y_2 (m)	F_{t1} (N)	F_{t2} (N)	\ddot{x}_s (m/s ²)	$\ddot{\theta}_s$ (rad/s ²)	F_{a1} (N)	F_{a2} (N)
Uncontrolled	0.0193	0.0097	520.45	285.29	1.0838	0.5216	–	–
PID	0.0093	0.0055	561.44	299.99	0.8638	0.7128	286.79	133.15
PID + SMRC	0.0230	0.0154	348.05	361.51	0.4568	0.6894	570.89	265.80

PID: proportional–integral–derivative; SMRC: sliding mode reference conditioning.

Table 5. Weighted RMS acceleration and corresponding discomfort level of passive and active suspension systems.

	a_w^{RMS} (m/s ²)	ISO 2631-1 discomfort level
Uncontrolled	0.5251	Fairly uncomfortable
PID	0.4323	A little uncomfortable
PID + SMRC	0.2401	Not uncomfortable

PID: proportional–integral–derivative; SMRC: sliding mode reference conditioning.

unlike the PID, the PID + SMRC algorithm is closer to this limit. Limit values used for the sprung mass vertical acceleration ($\pm 1.2 \text{ m/s}^2$) were selected to reduce the acceleration variation of the uncontrolled case. Figure 5 shows the vertical acceleration of the sprung mass, where limits used in the SMRC are marked as horizontal dashed lines. It is observed that between 1.1 and 1.72 s vertical acceleration restriction is performed by the SMRC algorithm three times. However, other limit values can be used considering that lower limits imply greater system forces and consequently, a greater energy demanded. Lower limits may also imply to not fulfill the maximum suspension deflection, and it could push to exceed the static tire load in detriment of a

good road holding. However, the limit could be relaxed as desired by the system designer, and the closed-loop response and energy requirement would tend to be the one of the PID controllers (without the SMRC loop).

Both PID and PID + SMRC algorithms show a good road holding since the dynamic tire load did not exceed the static tire load (F_{ti}^{stat}) in any case. According to equation (13) and model parameters of Table 3, the static tire load values for the front and rear are 2666 and 3803 N, respectively, while the maximum dynamic tire load obtained from the PID + SMRC algorithm were 1568 and 1363 N, respectively. Moreover, the dynamic tire load from the PID + SMRC algorithm is less than exhibited by the PID control (Figure 7).

The SMRC output performance shown in Figure 8 presents three events where the acceleration limits are prone to be exceeded: two for the upper limit (ω^+) and one for the lower limit (ω^-). This smoothed switching behavior of the SMRC algorithm was designed to modify the force demanded through the proportional term of the PID algorithm. Alternative paths of the SMRC algorithm to modify the PID output were tested but no improvements were achieved.

Unlike many papers that compare the performance of an advanced control strategy regards to a classical

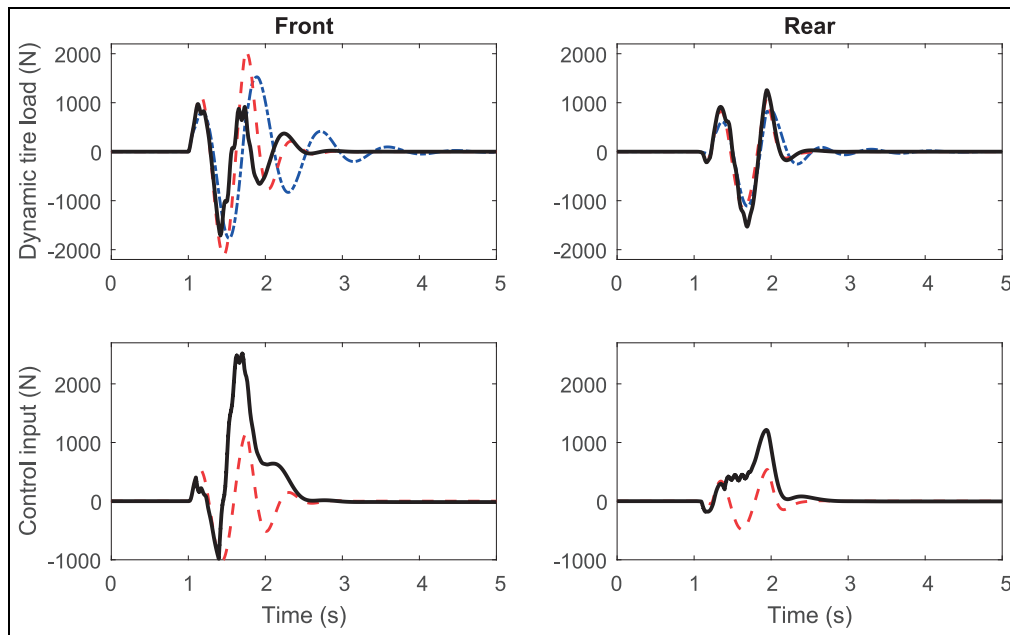


Figure 7. Dynamic tire load (top) from all suspension systems, and front and rear control inputs (bottom) performed by the PID and PID + SMRC control algorithms.

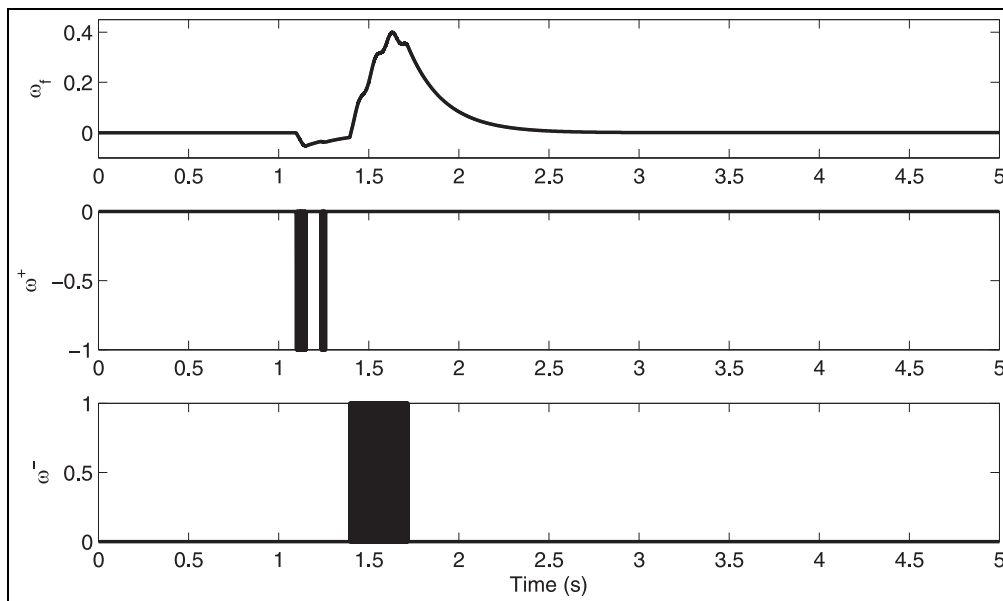


Figure 8. SMRC smoothed output (ω_f) performed for the bump disturbance, and resulting individual ω^+ (middle) and ω^- (bottom) signals for upper and lower limits of the sprung vertical acceleration.

Table 6. RMS values of the performance metrics from the PID + SMRC control using PID gains variations of Nominal + 30% and Nominal – 30%.

PID gains	γ_1 (m)	γ_2 (m)	F_{t1} (N)	F_{t2} (N)	\ddot{x}_s (m/s ²)	$\ddot{\theta}_s$ (rad/s ²)	F_{a1} (N)	F_{a2} (N)	d_w^{RMS} (m/s ²)
Nominal + 30%	0.0225	0.0149	355.53	366.34	0.4501	0.6996	571.56	279.77	0.2387
Nominal – 30%	0.0236	0.0161	337.30	355.69	0.4704	0.6745	568.73	250.87	0.2443

PID algorithm and whose improved results are subject to a particular tuning of the PID, here we have compared our strategy respect to the original PID

implementing the same tuning. This means that if the PID was poorly tuned, the performance of our proposal would be limited in the same way. However, an

outperformance was achieved in our active suspension control proposal improving the main controller used. In this regard, Table 6 shows the performance metrics obtained from the PID + SMRC control algorithm using PID gains variations of nominal + 30% and nominal – 30% values, which could represent an important source of uncertainty. It can be seen that the resulting performance is not affected by this PID gain variation, obtaining a discomfort level of “Not uncomfortable” according to the ISO 2631-1.

Conclusion

In this article, the SMRC control strategy was implemented on a PID control algorithm to improve the ride comfort experienced aboard a car. The external loop integrated by the SMRC algorithm allows reducing the level of discomfort likely reaction in 54.3% and 44.4% respect to the uncontrolled and PID cases, respectively. This improvement has been validated on a typical bump test, where the level of discomfort, according to ISO 2631-1:1997 assessment, is considered as not uncomfortable for the PID + SMRC, while fairly and little uncomfortable for the uncontrolled and the PID without SMRC cases, respectively. This improved performance does not affect the car safety since the PID + SMRC algorithm achieves good road holding evidenced by a lower dynamic tire load compared to the original PID control.


Declaration of conflicting interests

The author(s) declared no potential conflicts of interest with respect to the research, authorship, and/or publication of this article.

Funding

The author(s) disclosed receipt of the following financial support for the research, authorship, and/or publication of this article: This work has been supported by Universidad Antonio Nariño (20141110), Colombia, and by CONICET (PIP0837), MINCYT (PICT2394), and Universidad Nacional de La Plata (I216), Argentina.

ORCID iD

Fabian León-Vargas  <https://orcid.org/0000-0002-1839-2036>

References

1. Cao J, Liu H, Li P, et al. State of the art in vehicle active suspension adaptive control systems based on intelligent methodologies. *IEEE T Intell Transp* 2008; 9(3): 392–405.
2. Sun W, Gao H and Kaynak O. Adaptive backstepping control for active suspension systems with hard constraints. *IEEE/ASME T Mech* 2013; 18(3): 1072–1079.
3. Zapateiro M, Pozo F, Karimi HR, et al. Semiactive control methodologies for suspension control with magnetorheological dampers. *IEEE/ASME T Mech* 2012; 17(2): 370–380.
4. Foo E and Goodall RM. Active suspension control of flexible-bodied railway vehicles using electro-hydraulic and electro-magnetic actuators. *Control Eng Pract* 2000; 8: 507–518.
5. Gao B, Darling J, Tilley DG, et al. Control of a hydro-pneumatic active suspension based on a non-linear quarter-car model. *Proc IMechE, Part I: J Systems and Control Engineering* 2006; 220(1): 15–31.
6. Yagiz N and Hacıoglu Y. Backstepping control of a vehicle with active suspensions. *Control Eng Pract* 2008; 16: 1457–1467.
7. Du H and Zhang N. Fuzzy control for nonlinear uncertain electrohydraulic active suspensions with input constraint. *IEEE T Fuzzy Syst* 2009; 17(2): 343–356.
8. Wang YH and Shih MC. Design of a genetic-algorithm-based self-tuning sliding fuzzy controller for an active suspension system. *Proc IMechE, Part I: J Systems and Control Engineering* 2011; 225(3): 367–383.
9. Demir O, Keskin I and Cetin S. Modeling and control of a nonlinear half-vehicle suspension system: a hybrid fuzzy logic approach. *Nonlinear Dynam* 2012; 67: 2139–2151.
10. Li H, Yu J, Hilton C, et al. Adaptive sliding-mode control for nonlinear active suspension vehicle systems using T–S fuzzy approach. *IEEE T Ind Electron* 2013; 60(8): 3328–3338.
11. Gaspar P, Szaszi I, Balas GJ, et al. Design of robust controllers for active vehicle suspensions. In: *Proceedings of the IFAC world congress*, Barcelona, 21–26 July 2002, pp.1473–1478.
12. Du H and Zhang N. Constrained H_∞ control of active suspension for a half-car model with a time delay in control. *Proc IMechE, Part D: J Automobile Engineering* 2008; 222(5): 665–684.
13. Li H, Gao H, Liu H, et al. Fault-tolerant H_∞ control for active suspension vehicle systems with actuator faults. *Proc IMechE, Part I: J Systems and Control Engineering* 2011; 226(3): 348–363.
14. Li H, Liu H, Hilton C, et al. Non-fragile H_∞ control for half-vehicle active suspension systems with actuator uncertainties. *J Vib Control* 2012; 19(4): 560–575.
15. Gao H, Lam J and Wang C. Multi-objective control of vehicle active suspension systems via load-dependent controllers. *J Sound Vib* 2006; 290: 654–675.
16. Velagic J and Islamovic B. Flatness based control of nonlinear half-car active suspension system. In: *Proceedings of the 23rd Mediterranean conference on control and automation (MED)*, Torremolinos, 16–19 June 2015, pp.94–101. New York: IEEE.
17. Wang G, Chen C and Yu S. Optimization and static output-feedback control for half-car active suspensions with constrained information. *J Sound Vib* 2016; 387: 1–13.
18. Ekoru JE and Pedro JO. Proportional-integral-derivative control of nonlinear half-car electro-hydraulic suspension systems. *J Zhejiang Univ: Sc A* 2013; 14(6): 401–416.
19. Bello MM, Babwuro AY and Fatai S. Active suspension force control with electro-hydraulic actuator dynamics. *ARPN J Eng Appl Sci* 2015; 10(23): 17327–17331.

20. Talib MH and Darus IZ. Self-tuning PID controller for active suspension system with hydraulic actuator. In: *Proceedings of the IEEE symposium on computers and informatics*, Langkawi, Malaysia, 7–9 April 2013, pp.74–79. New York: IEEE.
21. Garelli F, Camocardi P and Mantz R. Variable structure strategy to avoid amplitude and rate saturation in pitch control of a wind turbine. *Int J Hydrogen Energ* 2010; 35(11): 5869–5875.
22. Garelli F, Gracia L, Sala A, et al. Sliding mode speed auto-regulation technique for robotic tracking. *Robot Auton Syst* 2011; 59: 519–529.
23. León-Vargas F, Garelli F, De Battista H, et al. Postprandial response improvement via safety layer in closed-loop blood glucose controllers. *Biomed Signal Proces* 2015; 16: 80–87.
24. Garelli F, Mantz R and De Battista H. *Advanced control for constrained processes and systems* (IET control engineering series). London: Institution of Engineering and Technology, 2011.
25. Sam YM and Osman JH. Modeling and control of the active suspension system using proportional integral sliding mode approach. *Asian J Control* 2005; 7(2): 91–98.
26. Zhao F, Dong M, Qin Y, et al. Adaptive neural-sliding mode control of active suspension system for camera stabilization. *Shock Vib* 2015; 2015: 542364-1–542364-8.
27. Wang G, Chen C and Yu S. Finite-time sliding mode tracking control for active suspension systems via extended super-twisting observer. *Proc IMechE, Part I: J Systems and Control Engineering* 2017; 231(6): 459–470.
28. Dangor M, Dahunsi OA, Pedro JO, et al. Evolutionary algorithm-based PID controller tuning for nonlinear quarter-car electrohydraulic vehicle suspensions. *Non-linear Dynam* 2014; 78: 2795–2810.
29. Mansfield NJ. *Human response to vibrations*. New York: CRC Press, 2005.
30. Zuo L and Nayfeh SA. Low order continuous-time filters for approximation of the ISO 2631-1 human vibration sensitivity weightings. *J Sound Vib* 2003; 265: 459–465.
31. Revert A, Garelli F, Pico J, et al. Safety auxiliary feedback element for the artificial pancreas in type 1 diabetes. *IEEE T Biomed Eng* 2013; 60(8): 2113–2122.